

# Foreign Object Debris Detection Using a 78 GHz Sensor with Cosec Antenna

P. Feil<sup>#1</sup>, A. Zeitler<sup>\*2</sup>, T.P. Nguyen<sup>\*3</sup>, Ch. Pichot<sup>\*4</sup>, C. Migliaccio<sup>\*5</sup>, W. Menzel<sup>#6</sup>,

<sup>#</sup>Institute of Microwave Techniques, University of Ulm

Albert-Einstein-Allee 41, 89081 Ulm, Germany

<sup>1</sup>peter.feil@uni-ulm.de

<sup>6</sup>wolfgang.menzel@uni-ulm.de

<sup>\*</sup> LEAT, University of Nice Sophia Antipolis

CNRS UMR 6071. 250 rue A. Einstein, 06560 Valbonne Cédex, France

<sup>2</sup>armin.zeitler@unice.fr

<sup>3</sup>truc-phong.nguyen@unice.fr

<sup>4</sup>christian.pichot@unice.fr

<sup>5</sup>claire.migliaccio@unice.fr

**Abstract**— This paper presents the results of FOD measurements conducted using a broadband 78 GHz radar sensor. Previous studies with a short-range setup up to 30 m showed promising results. However, to meet the requirements of the intended application, the range has to be increased significantly. As for all radar systems, the range can be extended by increasing the transmitted power and/or the antenna gain. In this work two different folded reflectarray antennas with a cosec-shaped pattern have been used to improve the system performance and range. Together with a CFAR (constant false alarm rate) algorithm and a moving target indication advances could be achieved compared to the previous setup.

## I. INTRODUCTION

Since the last decade, Foreign Object Debris (FOD) detection on airport runways has been increased incessantly. Among the existing systems, we find those based on optical sensors like CDD cameras [1] or Lidar [2], and those based on mm-wave radars [3-4]. The system described in [5], which contains both radar and camera, can be located along airport travel surfaces and provides the real-time interrogation, visualization and approval of detected FODs with high speed and high resolution. Some of the above-mentioned approaches have been evaluated by the Federal Aviation Administration (FAA) in order to develop performance standards for FOD detection systems [6].

In our last work, a compact and low-cost broadband 73–80 GHz mm-wave sensor was used for FOD detection applications. High sensitivity and simultaneous objects detection capabilities were shown with a short-range setup up to 30 m [7]. But an extension of the actual detection range is required by the intended application. As the power provided by off-the-shelf MMICs is limited, the range of the system can only be affected by the antenna characteristic.

In this paper, two different folded reflect array antennas with a cosec-shaped pattern have been used to improve the system performance and range. Together with a CFAR (constant false alarm rate) algorithm and a moving target

indication, advances were achieved compared to the previous setup.

Section II deals with the radar sensor, antenna, and the signal processing of the FOD detection setup. Section III treats the description and interpretation of the results issued from the tests performed on the Aix les Mille Airport in September 2009.

## II. RADAR SENSOR, SIGNAL PROCESSING, AND ANTENNA

### A. Sensor Overview and Signal Processing

The same FMCW (Frequency Modulated Continuous Wave) radar sensor as in the previous work [7] was used for the FOD measurements. It comprises a PLL-stabilized synthesizer and operates at frequencies from 73 GHz to 80 GHz. A block diagram of the sensor is shown in Fig. 1.

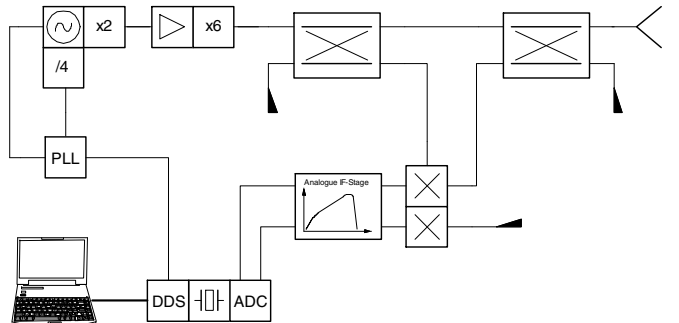


Fig. 1 Block diagram of the FMCW sensor used for foreign object detection.

As for most FMCW systems the range processing is done using a Fast Fourier Transform (FFT) of the intermediate frequency signal together with appropriate windowing. In addition, four subsequent measurements have been integrated to improve the signal to noise ratio.

A mechanical scanner was used for cross range imaging. The step size of the scanner was about 25% of the antennas' azimuthal beamwidth. This enables the application of an

angular moving average (MA) filter for additional noise reduction.

Due to the extended range compared to [7] the system requires about 20 dB increase in sensitivity. To achieve reliable object detection under low SNR conditions a two dimensional cell averaging CFAR algorithm was implemented according to [8]. The basic idea is to estimate the clutter and noise background by calculating the average power within a two dimensional window surrounding the resolution cell of interest (COI). Thereby the actual COI together with a small number of adjacent cells (“guard cells”) are excluded from the averaging.

The long-term stable synthesizer provides repeatable and phase stable measurements. A detected phase shift between two subsequent measurements indicates even sub-wavelength distance variations. This very simple kind of moving target indication was used to gain more information about the detected objects.

In addition, it was planned to perform a calibration measurement of the empty runway to further reduce clutter. Unfortunately, the cable shielding of one of the baseband connections was broken. Hence there was a strong interference by the airport radio, and the calibration measurements were corrupted.

### B. Antennas

To complete the sensor setup three different very compact folded reflect array antennas were attached to the mm-wave module.

The first antenna was the one used in [7], which provides a pencil beam radiation pattern. To increase the long range sensitivity and to properly use the dynamic range of the receiver, the received power  $P_{RX}$  must be kept constant for a target located at any distance on the runway. Therefore, two very compact folded reflect array antennas were developed to provide a constant  $P_{RX}$  between a distance range from 0.7 m up to 100 m due to a cosec-squared radiation pattern in elevation and a pencil beam pattern in azimuth.

The first proposed cosec antenna, described in [9], has a diameter of 12 cm (see Fig. 2); its average measured gain in the frequency range of interest is 33 dBi.

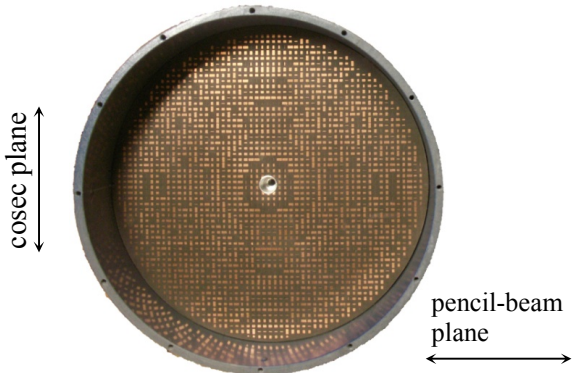


Fig. 2 Inlay of the small cosec antenna with the primary feed and definition of the planes.

Additionally, a second cosec antenna with a diameter of 20 cm was fabricated. As the distance between the transmitter and the receiver in the anechoic chamber was only 4.65 m, the condition for measurements in the far field of the antenna was not fulfilled and the measured gain and radiation pattern (Fig. 4) are drastically degraded. The simulated averaged gain is above 40 dBi, which is an improvement of 7 dB compared to the more compact reflect array antenna. The dimensions and the gain of the fabricated antennas are listed in Tab. I and the measured radiation patterns are presented in Fig. 3 and Fig. 4, respectively.

TABLE I  
DIMENSIONS AND AVERAGE GAIN OF THE FABRICATED ANTENNAS

	Antenna		
	Pencil Beam	Small Cosec	Large Cosec
Diameter	130 mm	120 mm	200 mm
Height	30 mm	32.5 mm	50 mm
Avg. Gain	34 dBi	33 dBi	40 dBi

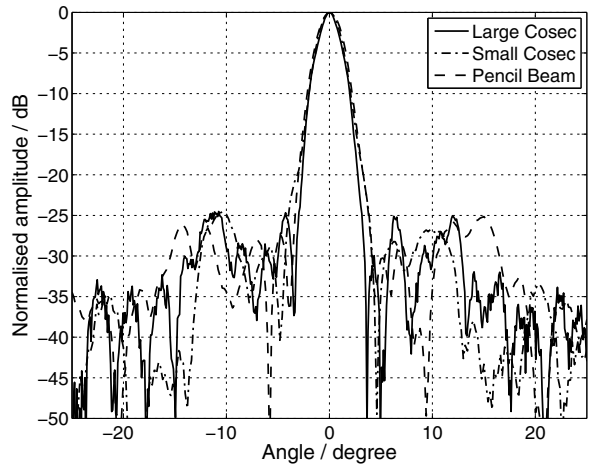


Fig. 3 Comparison of the measured radiation patterns in the pencil-beam plane for 78 GHz.

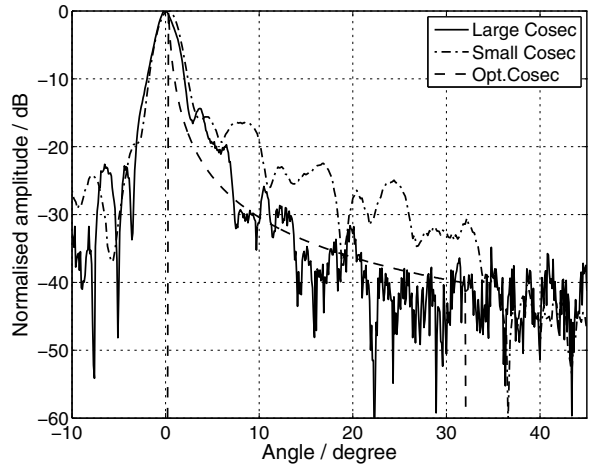


Fig. 4 Comparison of the measured radiation patterns in the cosec plane for 78 GHz and an optimal cosec pattern.

### III. MEASUREMENT RESULTS

#### A. Antenna Comparison

In a first step the performance of the different antennas with respect to  $P_{RX}$  over distance was estimated. The antennas were fixed on the turntable so that the maximum reflected power is received from an aluminum reflector on the runway 100 m away from the system. Then  $P_{RX}$  - reflected from a metal sphere with 40 mm diameter placed at different distances on the runway - was measured and is presented in Fig. 5. For comparison the calculated received power ( $P_{RX} \sim R^{-4}$ ) for a theoretical antenna, whose main beam is steered to each distance of interest is plotted as well as the  $P_{RX}$  for an antenna with an ideal cosec-squared radiation pattern.

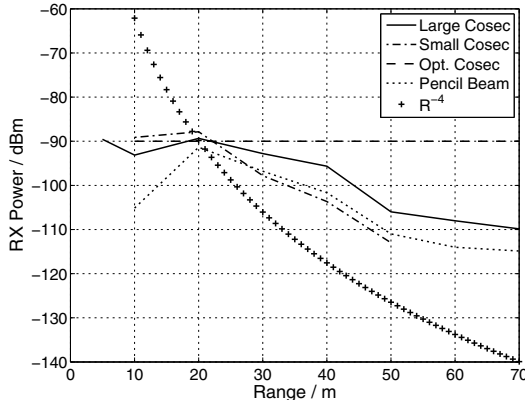


Fig. 5 Received power as a function of the distance for the three different antennas.

The variation in the received power for a theoretical antenna with constant gain would be more than 200 dB.

With the small cosec antenna the sphere in a distance larger than 50 m was not detectable and the variation in  $P_{RX}$  is 25 dB. For the pencil beam antenna the results vary between -115 dBm and -91 dBm which is a marginal benefit. The best results were obtained with the large cosec antenna as the sphere could be detected between a range of distance of 5 m to 70 m and the variation in power was 20.5 dB.

#### B. FOD Measurements

Radar measurements were taken in the same environment as in [7]. In addition to some reference targets such as spheres, also some real FODs collected at Charles de Gaulle Airport (CDG) have been used. A summary of all FOD's is given in Fig. 6 and Table II.



Fig. 6 Photograph of the FODs used for the measurements.

In the first scenario the FODs have been distributed randomly on the runway surface at distances up to 100 m. The sensor was located at the center of the runway and the antennas have been adjusted according to their design criteria with respect to maximum range and height over ground. The acquisition of the measurements and the processing of the data were done as described in Section II. The parameters of the CFAR target detection have been set to meet a reasonable trade-off between detection capability and false alarm rate.

Fig. 7 shows a photograph of the scenario from the sensor perspective. The position of the targets automatically detected using the large cosec antenna are superimposed. The evaluation was restricted to the region depicted by the blue line.

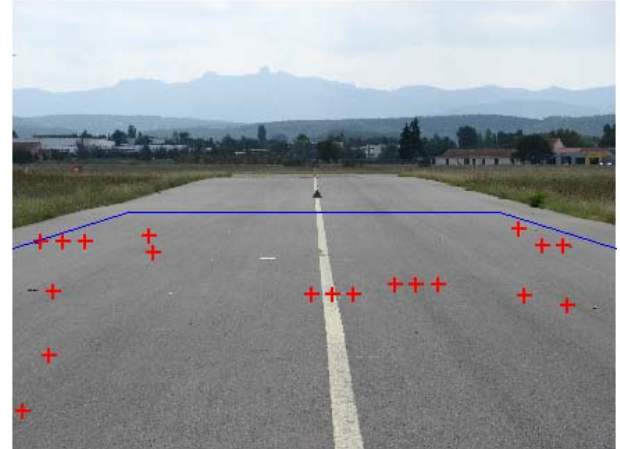


Fig. 7 Photograph of the scenario with superimposed FODs automatically detected with the large cosec antenna.

Due to the dense angular sampling and the implementation of the CFAR detector, objects can lead to a twofold and even threefold response.

Table II summarizes the detection results for the large cosec antenna (1), the small cosec antenna (2) and the pencil beam antenna (3).

TABLE II  
FOD DETECTION WITH DIFFERENT ANTENNAS

FOD No. and Description	R/m	Antenna		
		1	2	3
1 acrylic plate	40	N	N	N
2 sphere, 40 mm	55	Y	Y	Y
5 big stone	65	N	N	N
6 middle sized stone	32	Y	N	Y
7 small stone	29	N	N	Y
8 nut, M10	30	Y	N	Y
9 screw, M10 x 60 mm?	50	N	N	N
10 sphere, 25 mm?	30	Y	N	Y
11 piece of plane (CDG)	47	Y	Y	Y
12 plane tank cap (CDG)	50	Y	Y	Y
13 piece of plane break 1 (CDG)	32	Y	N	N
14 piece of plane break 2 (CDG)	74	N	N	N
15 piece of runway lamp 1 (CDG)	60	N	N	N
16 piece of runway lamp 2 (CDG)	31	N	Y	N
17 small stone (CDG)	29	Y	N	Y

The slope of the sensitivity (Fig. 4) is very similar for all antennas at distances larger than 20 m. Therefore, the detection capabilities are mainly determined by the antenna size and the maximum gain. As the large cosec antenna provides the highest gain, the detection rate is better compared to the other antennas. In spite of the significantly smaller diameter the performance of the pencil beam antenna gets very close. However, if FOD detection is needed very close to the sensor, the use of a cosec antenna is recommended. The minimum distance is given by the sensor arrangement. In [5] the sensors are placed directly at the runway border. The cosec antenna design in this paper assumes a sensor position about 1 m off the runway.

For the second scenario the sensor was placed beside the runway, about 15 m apart. The detection capabilities in this scenario were the same as for the first one. In addition, the moving target indication as described in Section II was evaluated. Thereby it was tried to detect a moving person at different positions on the runway. Fig. 8 shows the result of the measurement.

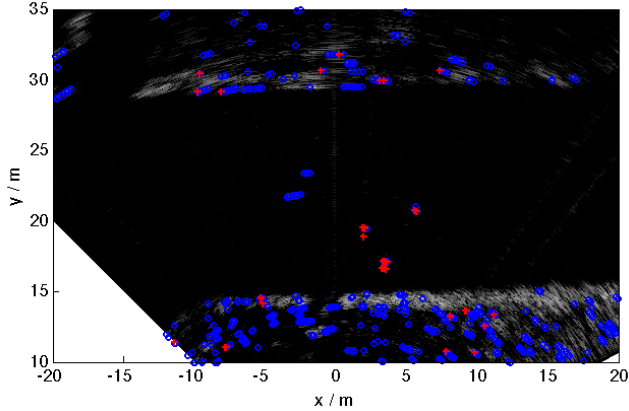


Fig. 8 Radar image of the second scenario with automatically detected static (blue) and moving (red) targets.

The radar image is superimposed with marks depicting targets detected by the CFAR algorithm. Static targets are indicated by blue markers and moving targets (with a minimum speed of 0.2 m/s) by red markers. Due to the wind the clutter introduced by the grass led to both moving and static targets. However, moving targets located on the runway can be clearly identified.

#### IV. CONCLUSIONS

A low power and broadband FOD detection radar using folded reflectarray antennas with cosec-pattern has been investigated. Especially at short ranges the use of cosec antennas is advantageous compared to pencil beam antennas. Provided a sufficient antenna gain and appropriate signal processing, it seems feasible to use such a setup up to 100 m. As the SNR was degraded by a broken shielding, the maximum range for given FODs have to be found out by additional measurement that will be taken within the next months. The results will be presented at the conference.

#### ACKNOWLEDGMENT

The authors would like to thank the French Civil Aviation for enabling the airport tests of Aix Les Milles.

#### REFERENCES

- [1] Stratech, iFerret system: [http://www.stratechsystems.com/iv\\_iferret.asp](http://www.stratechsystems.com/iv_iferret.asp).
- [2] LaserOptronix. <http://www.laseroptronix.se/airpor/airport.html>.
- [3] S.P Beasley, G. Binns, R. Hodges, R.J Badley, Tarsier, "A Millimetre Wave Radar for Airport Runway Debris Detection", in *Proc. of EURAD '04*, 2004, Amsterdam.
- [4] NAVTECH, <http://www.nav-tech.com/Runway%20Surveillance.htm>.
- [5] Xsight system: <http://www.xsightsys.com/index.aspx?id=3287>.
- [6] M. J. O'Donnell, "Foreign Object Debris/Damage (FOD) Detection Equipment", *Advisory circular of U.S department of transportation, Federal Aviation Administration, August 10 2009*.
- [7] P. Feil, W. Menzel, T.P. Nguyen, C. Pichot, and C. Migliaccio, "Foreign objects debris detection (FOD) on airport runways using a broadband 78 GHz sensor," in *Proc. European Radar Conference EuRAD 2008*, 2008, pp. 451-454.
- [8] H. Rohling, "Radar CFAR Thresholding in Clutter and Multiple Target Situations," *IEEE Transactions on Aerospace and Electronic Systems*, Vol. 19, pp. 8-621, 1983.
- [9] J. Lanteri, A. Zeitler, J.Y. Dauvignac, C. Pichot, C. Migliaccio, P. Feil, and W. Menzel, "Investigation of wideband millimetre-wave reflectarrays for radar applications operating in the W Band," in *Proc. 3rd European Conference on Antennas and Propagation EuCAP 2009*, 2009, pp. 826-830.